

Design and Simulation of Z-Source Inverter Fed Brushless DC Motor Drive Supplied With Fuel Cell for Automotive Applications

Mohsen Teimoori¹, Sayyed Hossein Edjtahed², Abolfazl Halvaei Niasar^{2*},

¹Department of Electrical Engineering, University of Allameh Feiz Kashani, Kashan, Iran

²Department of Electrical and Computer Engineering, University of Kashan, Kashan, Iran

Abstract

This paper presents design and simulation of Z-source inverter fed brushless DC motor drive supplied with fuel cell for automotive applications. The brushless DC (BLDC) motor are used due to many advantages such as high efficiency, high torque, high reliability, high-power density, lower maintenance compared to other motors in electric transport applications. The BLDC motor drive is with voltage source inverter (VSI) or current source inverter (CSI) because of low efficiency, high thermal loss, and inductor and capacitor large values inherently unreliable. Also shoot-through in DC bus in VSI and open circuit in DC link in CSI causes damage to the power source connected to the inverter, such as fuel cells, solar cells or the battery. In VSI and CSI are for increasing and decreasing the output voltage needs to separate DC-DC Buck and Boost converter. But their disadvantages have been overcome in the Z-source inverter using two inductors and capacitors. Also the Z-source inverter has inherent protection against shoot-through in the DC bus and boost voltage ability. In this paper the BLDC motor drive supplied to the fuel cell via a Z-source inverter are designed and evaluated. The simulation results show that the output voltage of fuel cell less can be settled in desired zone with changing capacitors and inductors and operating duty cycle.

Keywords: Brushless DC motor (BLDC), impedance source inverter (ZSI), fuel cell, Shoot-through duty cycle, conventional inverter

***Author for Correspondence** E-mail: halvaei@kashanu.ac.ir

INTRODUCTION

Electric motors have been known as one of the major consumers of electrical power today. The brushless DC (BLDC) motor is used because very high efficiency, high-power density and torque, simple structure, low maintenance costs and easy control method in automotive appliances, aerospace and industrial widely [1].

A brushless motor is a synchronous rotating machine, which has permanent magnet rotor and certain situations of rotating shaft rotor use for electronic commutation [2].

To rotate a BLDC motor stator windings should be energized according to the position of rotor, therefore knowing the information of the rotor angular position is essential to control BLDC motor drive. For this purpose, Hall-Effect sensors are generally used [3, 4].

Inverters are equipment that is used to convert direct current (DC) to alternating current (AC).

The voltage source inverter (VSI) has less output voltage than DC supply voltage [5], and to increase the output voltage the boost converter is needed.

Incurrent source inverter (CSI), output voltage is greater than DC supply voltage, and to reduce the output voltage, the buck converter is used. To overcome these problems impedance source inverter (ZSI) can be used [17].

It has many usages for increasing the output voltage and inherent protection against shoot-through in DC bus, high efficiency, drive strength, and reduce cost and size of the passive elements and the elimination of dead time.

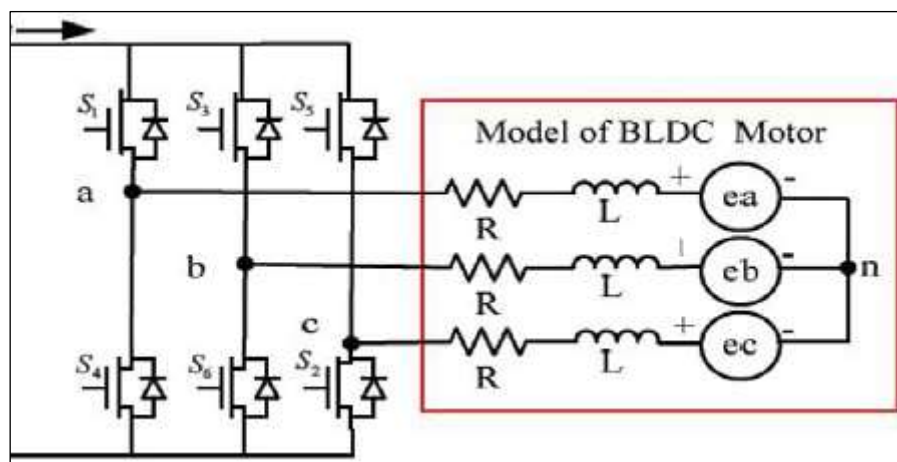


Fig. 1: Configuration of BLDC Motor Drive System

MODELING OF THE BRUSHLESS DC MOTOR

The BLDC motor is fed by a three-phase voltage source inverter as shown in Figure 1 [6].

So, the voltage equations will be following as:

$$V_a = Ri_a + (L - M)di_a/dt + e_a$$

$$V_b = Ri_b + (L - M)di_b/dt + e_b$$

$$V_c = Ri_c + (L - M)di_c/dt + e_c \quad (1)$$

Where V_a, V_b, V_c are the phase voltages, i_a, i_b, i_c are the phase currents, e_a, e_b, e_c are the phase back-EMF waveforms, R is the phase resistance, L is the phase inductance of each phase and M is the mutual inductance between any two phases. The electromagnetic torque is obtained as:

$$T_e = \frac{1}{\omega_r} (e_a i_a + e_b i_b + e_c i_c) \quad (2)$$

ω_r is the mechanic speed of the rotor and T_e is the electromagnetic torque. The equation of motion is:

$$\frac{d\omega_r}{dt} = \frac{1}{j} (T_e - T_L - B\omega_r) \quad (3)$$

B is the damping constant; j is the moment of inertia of the drive and T_L is the load torque [7, 8].

The Conventional Inverters Used in the BLDC Motor

The BLDC motor due to its electronically current commutation, as opposed to induction and synchronous motors even at constant

speed applications requires power converter (inverter). Structure of the VSI is composed which consists of a diode after of fuel cell, DC link capacitor, and inverter bridge. Structure of the CSI is composed which includes the diode after of fuel cell, which prevents reverse current through the fuel cell, The input to the inverter is a current source with an inductor in series, and inverter bridge. Both inverters are limitations and problems in common: [9–13]: Neither the voltage source converter main CSI can be used for the current source converter, or vice versa.

Fuel Cell Power Model

Fuel cell power plants are electrochemical devices that convert the chemical energy of a reaction directly into the electrical energy. There are different types of fuel cell and one of them the proton polymer fuel cell (PEMFC), because its membrane is small and light, working with low-temperature, solid electrolyte fuel cell and also due to its flexible electrolyte, the possibility of breaking or cracking is low, and so, PEMFC fuel cell is suitable for transportation applications. The fuel cell voltage and current fuel cell is generated fuel cell power. By increasing the load, it causes increasing the output current of fuel cell and reducing the output voltage of fuel cell. Figure 2 show the fuel cell voltage, current and power curves [14].

In next section brief acquaintance with and advantages of impedance source inverter ZSI is proposed and then the impedance source inverter ZSI used with the BLDC drive system connected with fuel cell is presented.

ZSI USED IN THE BLDC MOTOR DRIVE

Impedance source inverter ZSI is created using a unique impedance network cause creation a single-stage converter that can change output voltage from zero to infinity. The impedance networks is an effective tool for power conversion between source and load in a range limited in electric power conversion applications (DC-AC, AC-DC, AC-AC, DC-DC) [15], It is presented for different applications, different impedance source structure and various control procedures. There is possible operation impedance source inverter ZSI as buck, boost, unidirectional, bidirectional, isolated as well non-isolated [16]. The impedance source inverter ZSI overcome on problems and limitations mentioned for inverter VSI, CSI. The Z-network formed by the inductors L_1 and L_2 ,

and the capacitors C_1 and C_2 . The Z-network is symmetric, and acts as an intermediary between the load and source. Despite the symmetrical Z-network are equal values inductors and capacitors are equal. So they are equal inductor and capacitor voltages and inductor and capacitor currents together.

$$\begin{aligned} L_1 = L_2 = L, C_1 = C_2 = C \\ v_{L1} = v_{L2} = v_L, v_{C1} = v_{C2} = v_C \\ i_{L1} = i_{L2} = i_L, i_{C1} = i_{C2} = i_C \end{aligned} \quad (4)$$

A ZSI has three modes of operation: (1) active mode (A); when the VSI delivers an active voltage vectors, (2) open mode (O) when the VSI delivers a zero voltage vectors, and (3) shoot-through (T) or d_s mode when both the switches of one leg (or of all the three legs) of the VSI are ON simultaneously and the Z-link is short-circuited (Figure 3).

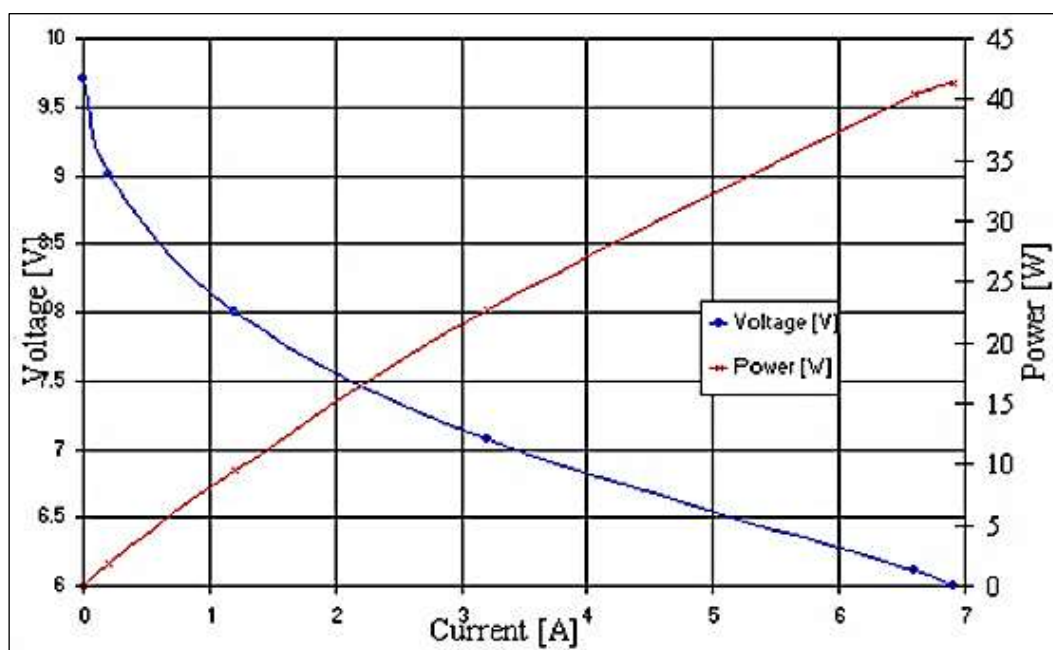


Fig. 2: P-I, V-I Curves of Fuel Cell.

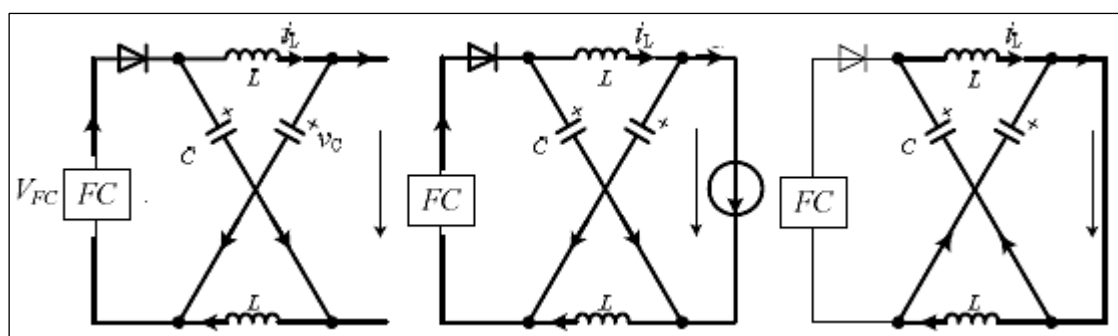


Fig. 3: Circuit of Z-source Network In (a) Open State (b) Active State (c) Shoot-through State.

A and O Modes are accomplished in a conventional VSI, while T mode is prohibited; here it is made possible by the Z-network. T Mode produces a zero voltage vector at the VSI output like O mode when the nominal voltage is required at the terminals of the VSI. Therefore, only A and T modes are considerate [17–23]. Figure 3 are shown different modes on the network impedance.

Figure 4 shows the schematic of a BLDC drive with the ZSI supply. In addition to the VSI, the impedance source inverter ZSI includes the diode D_s , which prevents reverse current through the fuel cell.

During A mode, the fuel cell power charges the capacitors C_1 and C_1 through the inductors L_1 and L_2 . Then the voltages across the capacitors increase whilst the currents into the inductors decrease. In correspondence, the energy stored into the capacitors increases whilst that one stored into the inductors decreases.

During mode T, the diode D_s is OFF since it is inversely biased by the voltage across the capacitors, thus isolating the fuel cell from the Z-network. Moreover, being the Z-link short-circuited, the couples of components L_1, C_2 and L_2, C_1 are connected in parallel and the increase of energy stored in the capacitors

during mode A is transferred to the inductors. Consequently, the voltages across the capacitors decrease and the currents in the inductors increase.

In steady state, equating to zero the balance of the energy stored in the inductors and inductors average voltage during T_S , yields. To obtain d_S the shoot-through time by given V_N the BLDC motor rated voltage and V_{FCN} nominal voltage of the fuel cell can be obtained from the following relationship [18].

$$V_N = \frac{1-d_S}{1-2d_S} V_{FCN} \tag{5}$$

And or:

$$d_S = \frac{V_N - V_{FCN}}{2V_N - V_{FCN}} \quad 0 < d_S < 0.5 \tag{6}$$

Where d_S is the value of shout-through time or shoot-through duty cycle. If $0 < d_S < 0.5$ so the shoot-through duty cycle provides the ability to boost voltage for BLDC motor drive system.

Shown in Figure 5 within a modulation period T_S , the duration of the shoot-through state and non-shoot-through state are T_{SH} and T_{NSH} thus ($T_{SH} + T_{NSH} = T_S$).

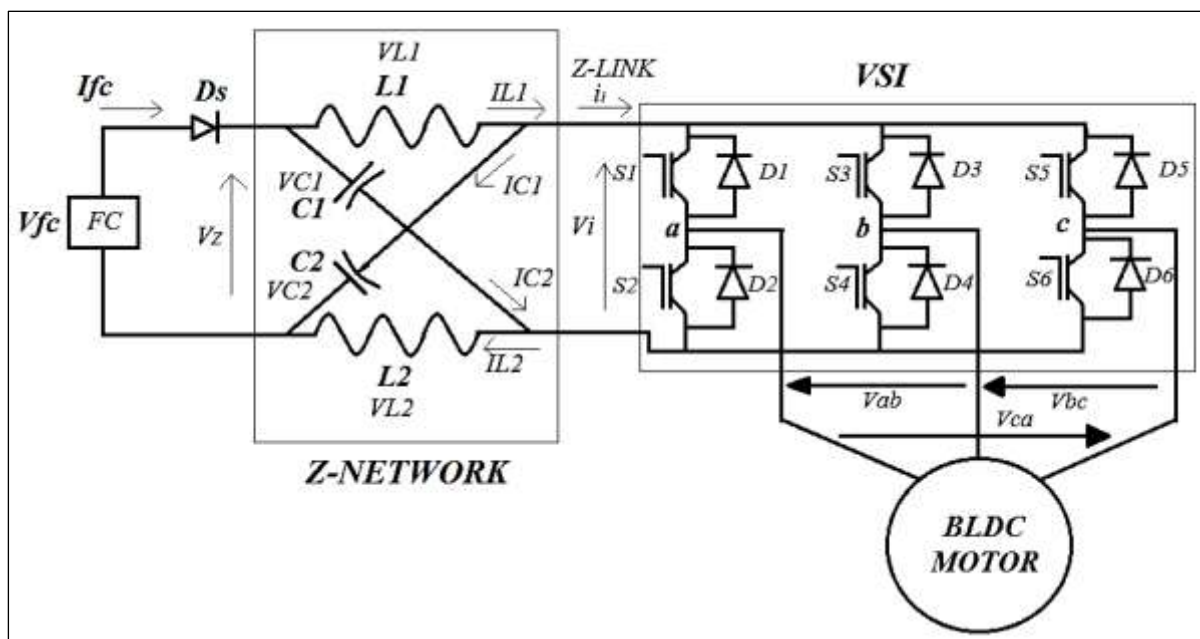


Fig. 4: BLDC Motor Drive with ZSI System.

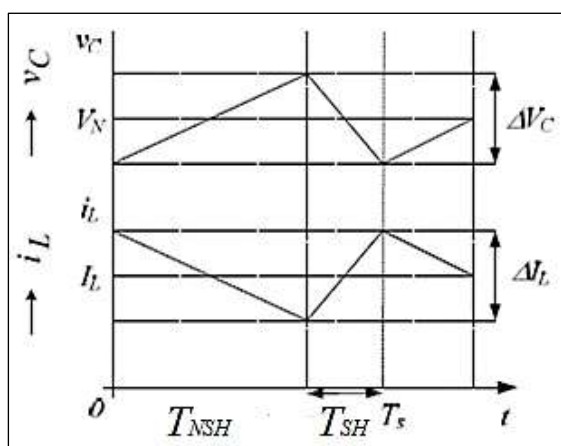


Fig. 5: Modulation Period T_S , Shoot-through State T_{SH} and Non-shoot-through State and T_{NSH} .

$$T_{SH} + T_{NSH} = T_S \quad (7)$$

that d_S shoot-through duty cycle is obtained from the following relationship:

$$d_S = \frac{T_{SH}}{T_S} \quad (8)$$

where G is the BLDC motor rated voltage ratio to fuel cell nominal voltage that is always greater than or equal to one.

$$G = \frac{V_N}{V_{FCN}} > 1 \quad (9)$$

or:

$$G = \frac{1-d_S}{1-2d_S} \quad (10)$$

The current i_i of the Z-link can be obtained after impedance network in figure from:

$$i_i = \begin{cases} I & \text{mode A} \\ i_t = 2i_L & \text{mode T} \end{cases} \quad (11)$$

That i_t is the shoot-through current. This impedance source inverter ZSI network effective as the energy storage or filtering inductor and capacitor elements for the impedance source inverter. This is more effective to minimize the voltage and current ripples. Another advantage is that in impedance source inverter ZSI, the value of inductor and capacitor should be smaller than traditional inverters.

DESIGN OF Z-SOURCE INVERTER

In proposed impedance source inverter ZSI, the passive components are designed according to T_S switching frequency, their

voltage ripple, current ripple, d_S , and inductors average nominal current and BLDC motor nominal voltage. The voltage ripple across the capacitor can be obtained in the ZSI according to Figure 5 the following relationship [24]:

$$\Delta V_C = \frac{I_{LN} T_S}{C} d_S \quad (12)$$

that T_S is the switching time; d_S is the shoot-through duty cycle. I_{LN} is the nominal average inductor current, and the current ripple through the inductor is:

$$\Delta I_L = \frac{V_N T_S}{L} d_S \quad (13)$$

and values inductor and capacitor can be obtained in the impedance network as function of switching frequency T_S , G , capacitor voltage ripple, inductor current ripple, inductor average nominal current and BLDC motor rate voltage from the following relationships:

$$L = \frac{V_N T_S}{I_{LN} r_i} \frac{G-1}{2G-1} \quad (14)$$

$$C = \frac{I_{LN} T_S}{V_N r_v} \frac{G-1}{2G-1} \quad (15)$$

The values of inductors and capacitors come out from the specifications on the allowed excursions of current in the inductors and of voltage across the capacitors. The specifications are aimed at keeping optimal the performance of the supplies and low the losses in the components. Furthermore, they help reducing the ripple of current into the fuel cell, so as to avoid a shortage of their life time. The specifications are given in terms of ripple of current into the inductors, r_i , and ripple of voltage across the capacitors, r_v is:

$$r_i = \frac{\Delta I_L}{I_{LN}}; \quad r_v = \frac{\Delta V_C}{V_N} \quad (16)$$

That the nominal value of current through the average inductors I_{LN} and ΔI_L and ΔV_C are the specified peak-to-peak excursions of current and voltage are determined [25].

How Operation Shoot-through d_S in the Impedance Source Inverter (ZSI)

The impedance source inverter ZSI is three-phase has six switches. And each leg has two switches that is one of the above leg S_1 and

another one lower leg S_2 . When the fuel cell output voltage is less than the rated voltage of BLDC motors and acted $d_s > 0$ and triangular pulse compared with $1 - d_s < 1$ such as occur shoot-through (T) mode and both S_1, S_2 activated.

When the fuel cell output voltage is equal to the rated voltage BLDC motors and acted $d_s = 0$ and triangular pulse compared with $1 - d_s < 1$ such as occurs activate (A) mode, and only S_2 is deactivated and S_1 is activated.

Therefore $0 < d_s < 0.5$ is limited and whatever d_s is more and has been short-through bandwidth more and period of time will be short-through switches S_1 and S_2 more and vice versa. For another legs, S_3, S_4, S_5 and S_6 act as in the first leg. Figure 6 shows how operation shoot-through d_s in the impedance source inverter ZSI.

SIMULATION RESULTS

The simulation block diagram of the impedance source inverter (ZSI) fed brushless dc motor drive supplied with fuel cell is shown in Figure 7. It has been taken diode and fuel cell before impedance source inverter ZSI and

the BLDC motors after the fuel cell. Figure 8 shows the motor drive system. In Figure 8, position sensors are considered to calculate the speed and is sent to speed controller. The current controller generates the three-phase currents commands to power inverter.

On the other hand d_s is adjusted by comparing fuel cell nominal voltage and the rated voltage BLDC motor according to equation (6) and comparing with PWM. In case that fuel cell voltage is less than the rated voltage, it acts shoot-through duty cycle command to power inverter pulse. The simulation models have been established using MATLAB/Simulink software. This simulation runs time for 0.5 seconds.

At first, speed of BLDC motor increase to 0.25 seconds as dip 1/4 slowly and after that, it will continue with reference speed 1400 rad/s and rated voltage 310 V.

The waveforms of the stator phase current, BLDC motor voltage, voltage before and after Z-network circuit, voltage back-EMF, rotor speed, torque are observed. Motor specifications and simulation parameters is given in Table 1.

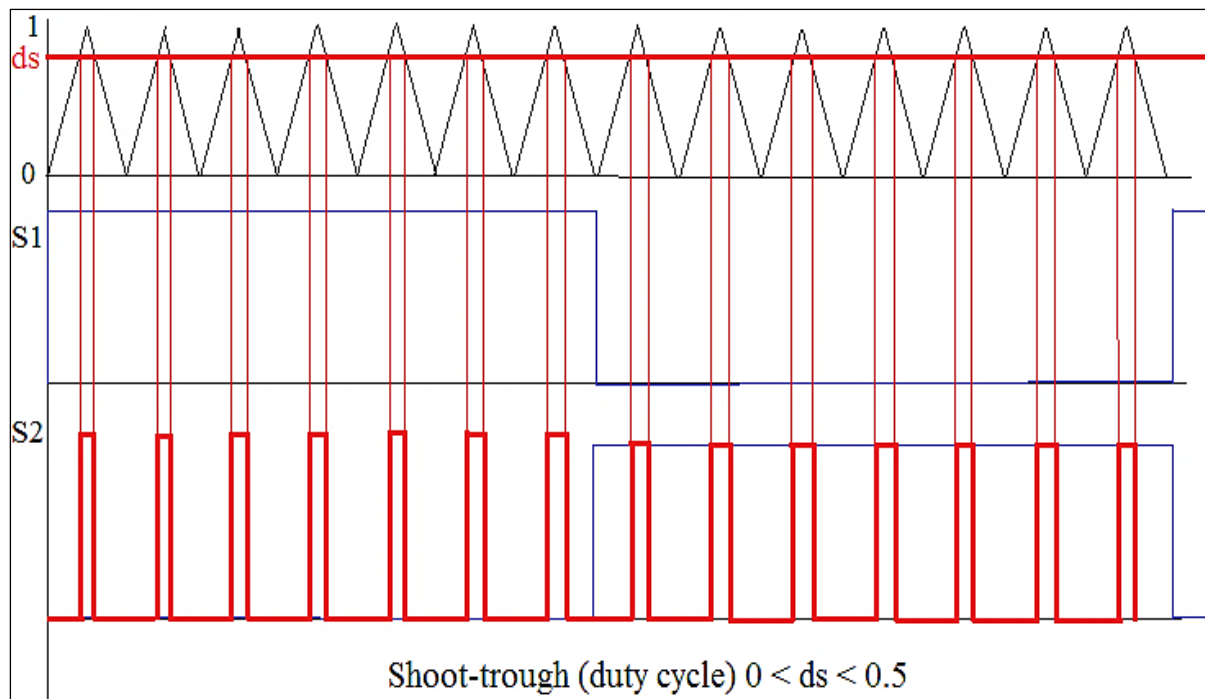


Fig. 6: Determination of Shoot-through d_s in ZSI.

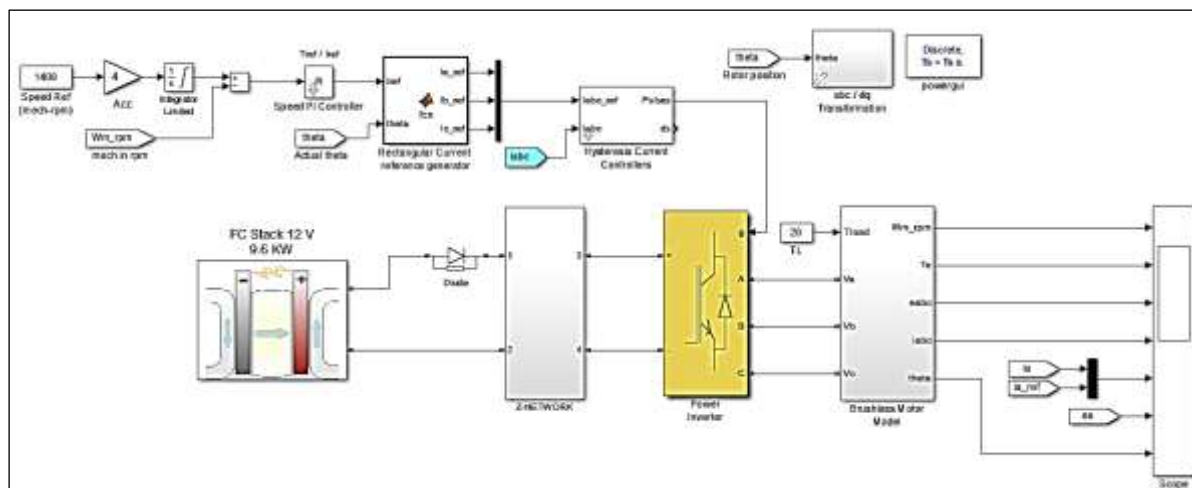


Fig. 7: Simulation of Z-source Inverter Fed Brushless DC Motor Drive Fed with Fuel Cell.

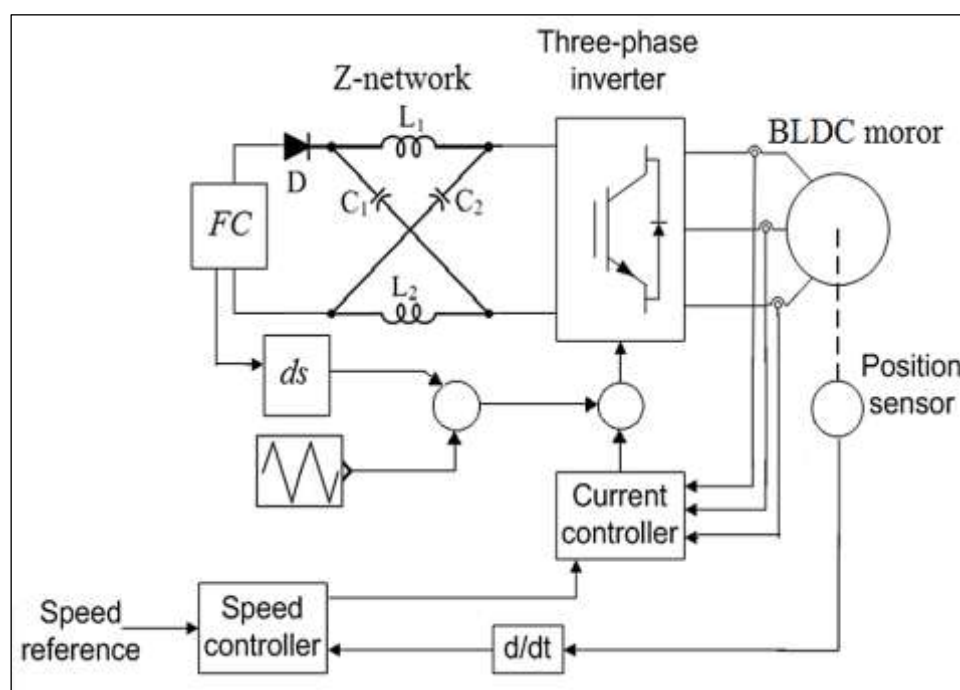


Fig. 8: Motor Drive System.

The aim of this simulation that with fuel cell voltage decrease and stay constant inverter output voltage or rated motor BLDC, rotor speed and rated torque makes that according to equation (6) changes automatically and values inductor and capacitor should be changed.

Two examples of simulation has been done and in finally, Table 2 results several example of simulation examination is shown full with different fuel cell voltages and powers and answer values inductor, capacitor, capacitor voltage, average inductor current, d_s and stator phase current.

Table 1: Simulation Parameters.

PARAMETER	VALUES
Rated rotor speed	1400 rpm
Motor rated voltage	$V_N = 310$ V
Frequency switching	$F_z = 25000$ Hz
Load torque	20 Nm
Fuel cell nominal voltage	41 V, 12 V
Motor stator phase resistance	0.19 Ω
Motor stator phase inductance	750 μH
Motor Mutual inductance	80 μH
Drive instant inertia	0.015
Number poles	12
Constant friction factor	0.00136

In the first simulation, is adjusted with fuel cell rated voltage = 41 V, fuel cell current = 350 A equal with fuel cell power = 14 kW, $L=10 \mu\text{H}$, $C=1000 \mu\text{F}$, $F_z = 25000 \text{ Hz}$ and in result $d_s = 0.458$, remain constant motor rated voltage, rotor speed and torque and is given Figures [9–11].

In this simulation, Figure 9 shows that despite shoot-through d_s and adjustment value inductance and capacitance thus increase the amplitude of BLDC motor line-to-line voltage before 0.25 seconds with slope 1/4 slowly and remain constant after 0.25 seconds 310 V. It is zoomed in Figure 10.

Figure 9(b) shows the amplitude of the back-EMF that despite shoot-through d_s and adjustment value inductance and capacitance thus value increase before 0.25 seconds with slope 1/4 slowly and is shown constant after 0.25 seconds 134 V.

Figure 9(c) shows voltage after impedance Z-network circuit (red) with 335 V is lower ripple ratio to before impedance Z-network circuit (blue) with 310 V despite value the capacitor. Voltage after Z impedance network circuit is always greater than before Z impedance network circuit.

Figure 11(a) shows despite shoot-through d_s and adjustment value inductor and capacitor thus waveform stator phase current is shown before 0.25 second with 18 A and after 0.25 second with 15 A. Figure 11(b) also shows load torque despite shoot-through d_s and adjustment value inductor and capacitor thus before 0.25 second with 30 Nm and load torque after 0.25 second with 20 Nm is shown. Figure 11(c) shows speed rotor is shown that despite shoot-through d_s and adjustment value inductance and capacitance thus increase before 0.25 seconds with slope 1/4 slowly and constant after 0.25 seconds with rotor speed 1400 rpm.

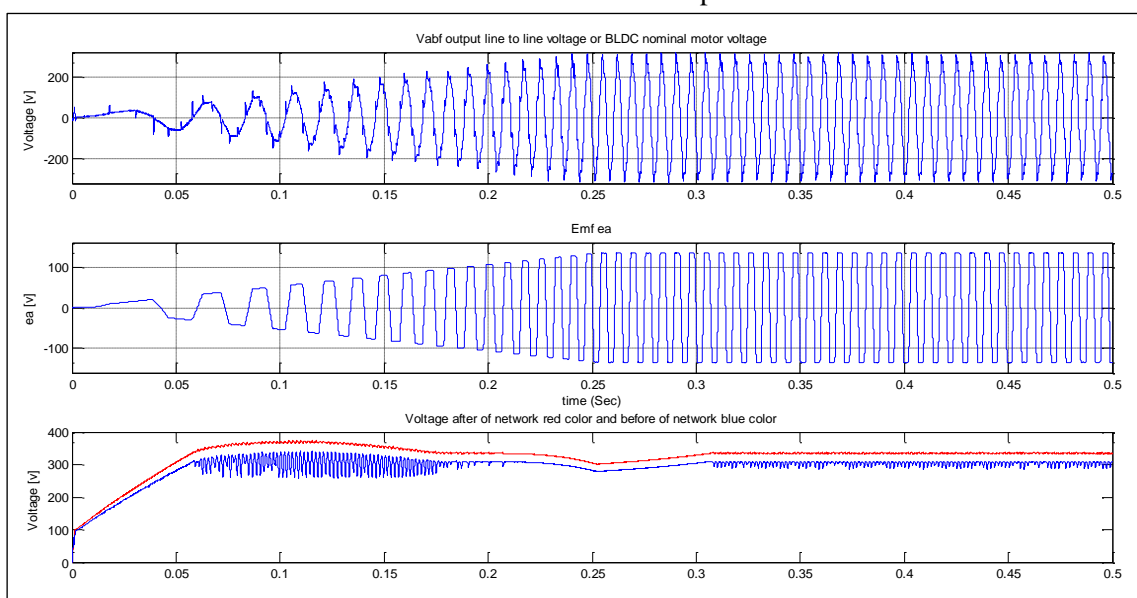


Fig. 9: (a) to (c) Voltage After and Before Z-network Circuit—Back-EMF—BLDC Motor Voltage.

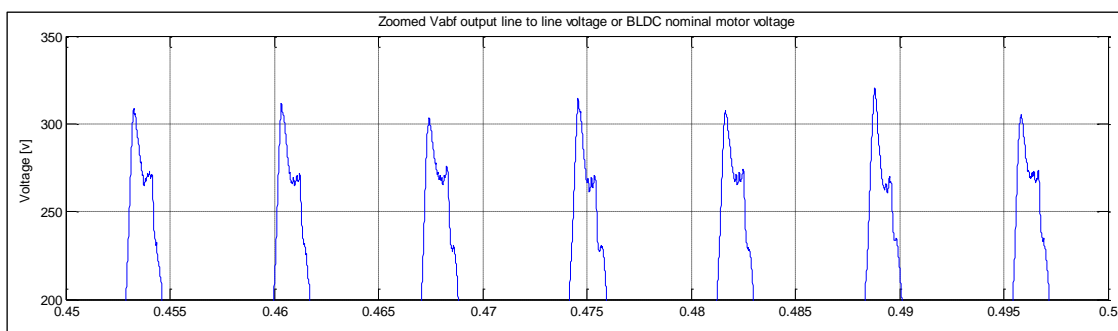


Fig. 10: Zoom of BLDC Motor line-to-line Voltage in 41 V.

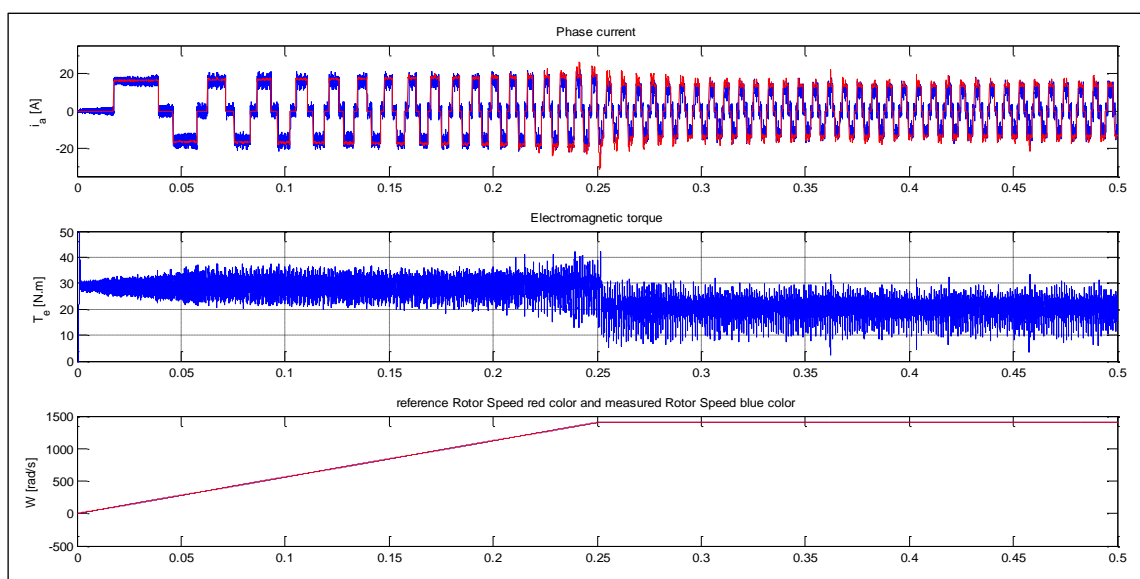


Fig. 11: (a) to (c) Waveforms of Rotor Speed, Torque, Stator Phase Current in 41 V.

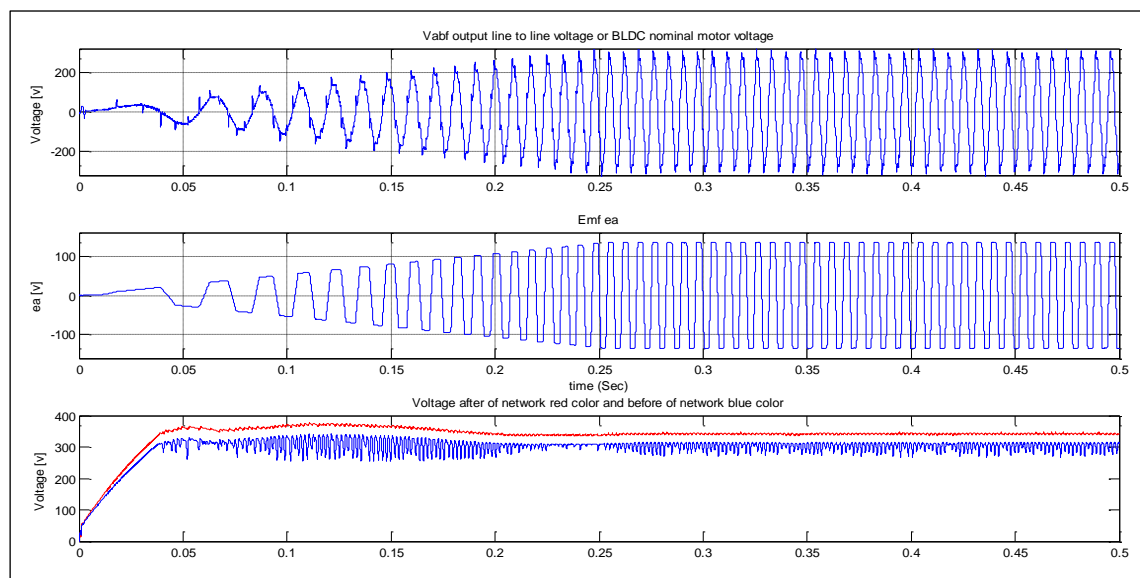


Fig. 12: (a) to (c) Voltage After and Before Z-network Circuit in 12 V.

In the second simulation, it is adjusted with fuel cell rated voltage = 12 V, fuel cell current = 800 A equal with fuel cell power = 9.6 kW, $L=2 \mu\text{H}$, $C=1000 \mu\text{F}$, $F_z = 25000 \text{ Hz}$ and in result $d_s = 0.49$, remain constant. motor rated voltage, rotor speed and torque and are given Figures [12–14].

This simulation examination shown in Figure 12(a) that despite shoot-through d_s and adjustment value inductance and capacitance thus increase the amplitude of BLDC motor line-to-line voltage before 0.25 seconds with slope 1/4 slowly and remain constant after

0.25 seconds 310 V. It is zoomed in Figure 13. Figure 12(b) which shows the amplitude of the back-EMF that despite shoot-through d_s and adjustment value inductance and capacitance thus value increase before 0.25 seconds with slope 1/4 slowly and is shown constant after 0.25 seconds 134 V.

Figure 12(c) shows voltage after impedance Z-network circuit (red) with 340 V is lower ripple ratio to before impedance Z-network circuit (blue) with 310 V despite value the capacitor. Voltage always after Z impedance network circuit is greater than before Z impedance network circuit.

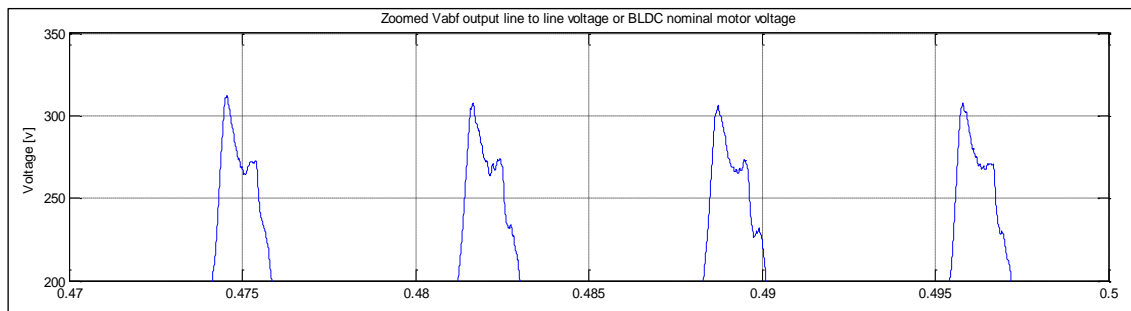


Fig. 13: BLDC Motor Line-to-line Voltage (Zoom) (12 V).

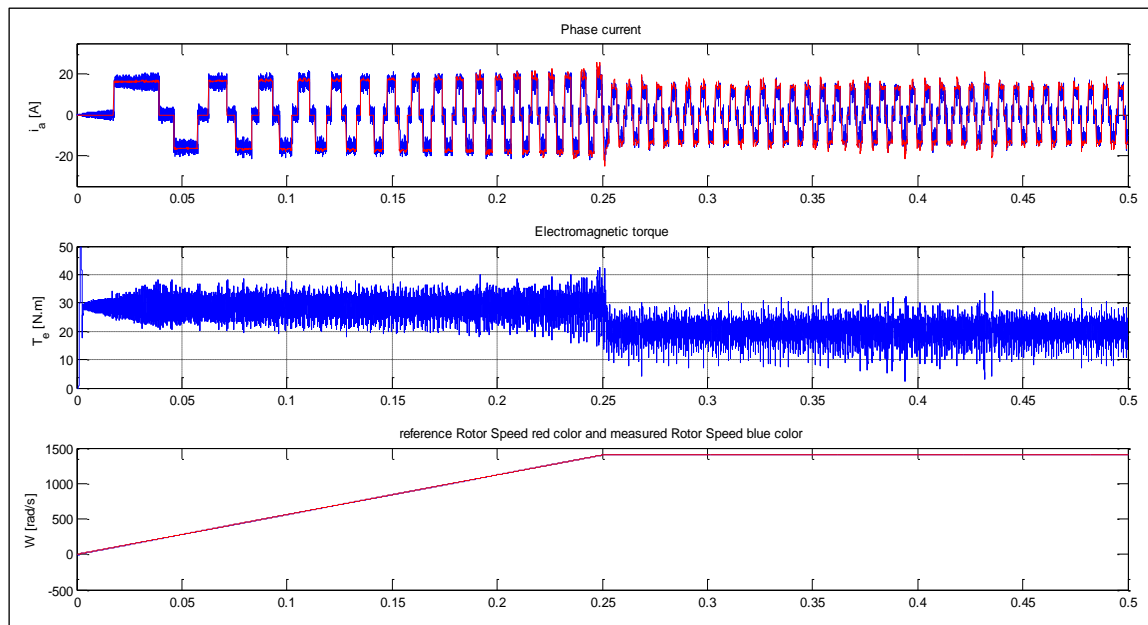


Fig. 14: (a) to (c) Waveform of Speed, Torque, Stator Phase Current in 12 V.

Table 2: The Simulation Examination Results.

FUEL CELL POWER PARAMETERS	$V_{fcN}=12\text{ V}$ $I_{fcN}=800\text{ A}$ $P_{fcN}=9.6\text{ kW}$	24 V 400 A 9.6 kW	41 V 350 A 14 kW	90 V 220 A 19.8 kW	120 V 250 A 30 kW	150 V 200 A 30 kW	180 V 180 A 27 kW	240 V 210 A 50 kW
L(μH)	2	7	10	22	34	400	400	500
C(μF)	1000	1000	1000	1000	1000	1000	900	500
Vc(V)	340	335	335	330	325	300	320	320
$i_L(\text{A})$ Average	222	80	55	23	17	16	16	16
Speed(rpm)	1400	1400	1400	1400	1400	1400	1400	1400
Torque(Nm)	20	20	20	20	20	20	20	20
Voltage line-to-line BLDC motor (V)	310	310	310	310	310	310	310	310
Voltage phase motor (V)	160	160	160	160	160	160	160	160
Back-EMF voltage (V)	134	134	134	134	134	134	134	134
d_s	0.49	0.47	0.458	0.406	0.345	0.26	0.175	0.005
Phase current (A)	14	14	15	15	15.5	16	16	16
$V_{fc}(\text{V})$	15	35.5	48	98	145	199	240	300
$I_{fc}(\text{A})$	222	80	60	30	25	16	15	15

Figure 14(a) shows despite shoot-through d_s and adjustment value inductor and capacitor thus waveform stator phase current is shown before 0.25 second with 18 A and after 0.25 second with 15 A. Figure 14(b) also shows load torque despite shoot-through d_s and adjustment value inductor and capacitor thus before 0.25 second with 30 Nm and load torque after 0.25 second with 20 Nm is shown.

Figure 14(c) shows speed rotor is shown that despite shoot-through d_s and adjustment value inductance and capacitance thus increase before 0.25 seconds with slope 1/4 slowly and constant after 0.25 seconds with rotor speed 1400 rpm.

CONCLUSION

This paper has proposed a novel electric drive system for impedance source inverter ZSI fed brushless DC motor drive supplied with fuel cell for automotive applications. It is concluded from the simulation examinations in Table 2 that when the fuel cell rated voltage is less than the motor rated voltage BLDC, cause performance shoot-through duty cycle d_s and along with adjusting the value of inductor and capacitor and switching frequency makes that is produced desirable impedance source inverter ZSI output voltage and BLDC motor rated voltage.

So, the fuel cell rated power is greater or equal with BLDC motor rated power until produces stable and desire the capacitor voltage V_c , rotor speed, load torque and stator phase currents, and is ability to increase and decrease the output voltage without additional converter. This drive many advantages are compared with conventional inverter including reducing price, increasing efficiency, reducing losses, reducing complexity design and elements for converters and inverters, reducing capacitor and inductor values. and also impedance source inverter ZSI has been possible shoot-through in circuit and inherent protection from shoot-through in the DC bus.

Overall result of this paper is inferred that operation shoot-through d_s duty cycle, adjustment switching frequency value and inductor and capacitor are three important factors to produce desirable output voltage.

REFERENCES

1. Millner AR. Multi-hundred horsepower permanent magnet brushless disc motors. *Applied Power Electronics Conference and Exposition*. 1994; 351–355p.
2. Lee BK and Ehsani M. Advanced BLDC Motor Drive for Low Cost and High Performance Propulsion System in Electric and Hybrid Vehicles. *IEEE 2001 International Electric Machines and Drives Conference*, 2001, Cambridge, MA, June 2001; 246–251p.
3. Rajashekara K, Kawamura A. Sensorless Control of Permanent Magnet AC Motors. 20th international *Conference on Industrial Electronics, Control and instrumentation*. IECON '94. 1994; 3: 1589–1594p.
4. Johnson JP, Ehsani M, Guzelgunler Y. Review of Sensorless Methods for Brushless DC. *Industry Applications Conference*. Thirty-Fourth IAS Annual Meeting. 1999; 1: 143–150p.
5. Bose BK. *Modern power electronics and AC drives*. Prentice Hall, Upper Saddle River, 2002.
6. Kenjo T and Nagamori S. *Permanent Magnet Brushless DC Motors*, Clarendon Press, Oxford, 1985.
7. Gieras JF and Wing M. *Permanent Magnet Motor Technology—Design and Application*, Marcel Dekker Inc., New York, 2002.
8. Niasar HA, Moghbelli H, Vahedi A. Modeling and Simulation Methods for Brushless DC Motor Drives. *International Conf. on Modeling, Simulation and Applied Optimization (ICMSAO)*. 2005; 05-70/05-176p.
9. Olzwesky M. Z-Source Inverter for Fuel Cell Vehicles. US Department of Energy, Freedom CAR and Vehicles Technologies, EE-2G, Washington, 2005.
10. Holland K, Shen M, Peng FZ. Z-Source Inverter Control for Traction Drive of Fuel Cell-Battery Hybrid Vehicles. *Industry Applications Conference*, 40th IAS Annual Meeting. 2005; 3(4): 1651–1656p.
11. Fang I and Peng Z. Z-Source Inverter. *IEEE Transactions Industry Applications*. 2003; 39(2): 990–997p.

12. Yunus HI, and Bass. Comparison of VSI and CSI topologies for single-phase active power filters. *Power Electronics Specialists Conference*. 1996; 2: 1892–1898p.
13. Hung-Chi Chen, and Hung-He Huang. Speed control for buck-type current source inverter fed BDCM without position sensors. *Industrial Electronics (ISIE)*, Taipei, Taiwan, 2013.
14. Chan C. The state of the art of electric, hybrid, and fuel cell vehicles. *Proceedings of the IEEE*. 2007; 95(4): 704–718p.
15. Fang Zheng Peng. Z-source inverter. *IEEE Transaction on Industry Application*. April 2003; 39:
16. Miaosen Shen, Jin Wang, Alan Joseph, Peng FZ, Leon M. Tolbert, and Donald J. Adams. Maximum Constant Boost Control of the Z-Source Inverter. Michigan State University.
17. Mazumdar J, Batarseh I, Kutkut N, Demirc O. High frequency low cost DC-AC inverter design with fuel cell source for home applications. *In Proc. IEEE IAS'02*. 2002; 789–794p.
18. Peng FZ. Z-source inverter. *IEEE Transactions on Industry Applications*. 2003; 39(2): 504–510p.
19. Shen M, Wang J, Joseph A, Peng F.-Z, Tolbert L, Adams D. Constant boost control of the z-source inverter to minimize current ripple and voltage stress. *IEEE Transactions on Industry Applications*. 2006; 42(3): 770–778p.
20. Shen M, Wang J, Joseph A, Peng F.-Z, Adams D. Comparison of traditional inverters and z-source inverter for fuel cell vehicles. *IEEE Transactions on Power Electronics*. 2007; 42(4): 1453–1463p.
21. Peng FZ, Shen M, Holland K. Application of z-source inverter for traction drive of fuel cell battery hybrid electric vehicles. *IEEE Transactions on Power Electronics*. 2007; 22(3): 1054–1061p.
22. Peng FZ, Joseph A, Wang J, Shen M, Chen L, Pan Z, Ortiz-Rivera E, Huang Y. Z-source inverter for motor drives. *IEEE Transactions on Power Electronics*. 2005; 22(4): 857–863p.
23. Rashid M. Power electronics: circuits, devices and applications. Pearson Prentice Hall, Upper Saddle River, 2004.
24. Peng FZ, Shen M, Holland K. Application of z-source inverter for traction drive of fuel cell battery hybrid electric vehicles. *IEEE Transactions on Power Electronics*. 2007; 22(3): 1054–1061p.
25. Buja G, Keshri RK, Roberto Menis. Comparison of DBI and ZSI Supply for PM Brushless DC Drives Powered by Fuel Cell. Department of Electrical Engineering, University of Padova, Italy, *IEEE Transactions on Power Electronics*. 2011; 165–170p.

Cite this Article

Mohsen Teimoori, Sayyed Hossein Edjtahed, Abolfazl Halvaei Niasar. Design and Simulation of Z-Source Inverter Fed Brushless DC Motor Drive Supplied With Fuel Cell for Automotive Applications. *Journal of Power Electronics and Power Systems*. 2016; 6(3): 60–71p.